Course Project Report

PH-819: Advanced Astrophysics

Rayleigh-Taylor Instability in Stellar Interiors

Group-I

Yugesh Bhoge, Lucky Chaudhary, Vasudev Dubey

23N0278, 24D1052, 23N0303

Submitted to: Prof. Rahul Kashyap

Department of Physics

Indian Institute of Technology Bombay

April 26, 2025

Abstract

The Rayleigh-Taylor Instability (RTI) arises when a denser fluid is supported against gravity by a lighter fluid, leading to interfacial perturbations that grow with time. This phenomenon is crucial in various astrophysical scenarios such as supernova remnants, stellar convection zones, and accretion disks. In this study, we analytically investigate the behaviour of RTI under the influence of magnetic fields using the framework of ideal magneto-hydrodynamics (MHD). Through linear stability analysis, we explore different configurations involving constant and non-uniform magnetic fields and density profiles. We derive generalised dispersion relations and analyse how magnetic tension modifies the growth rate of instabilities. Additionally, we implement a two-dimensional finite-volume simulation of the compressible Euler equations with gravity to visualise the nonlinear evolution of RTI. Our results confirm the stabilising influence of magnetic fields, especially for shorter wavelengths, and highlight conditions under which RTI is suppressed. These insights have implications for interpreting mixing processes in stellar environments and improving models of astrophysical plasma dynamics.

Contents

Chapter 1

Introduction

Everything in the universe tries to be in equilibrium, particularly stable equilibrium. But due to various environmental conditions, internal & external influences, the system can be pushed into states of instability. One such instability is the **Rayleigh-Taylor Instability (RTI)**, which occurs when a high-density fluid is accelerated into a low-density fluid under the influence of gravity. Another similar but different type of instability is **Kelvin-Helmholtz Instability (KHI)**, which is driven by the horizontal velocity gradient in the flow.

These instabilities are significant in astrophysical contexts such as core-collapse supernovae. The inner higher-density elements burst out in the lighter outer stellar atmosphere. This leads to the formation of mixing patterns which further shows the observable properties of supernova remnants. Understanding this process is essential, as we can interpret astronomical observations and also refine the stellar explosion models[1].

This project focuses mainly on the RTI and aims to answer the following questions:

- Why Rayleigh-Taylor Instability occur in the stellar interior?
- What we can infer by studying Rayleigh-Taylor Instability?
- What are the factors that affect Rayleigh-Taylor Instability?
- What are the effects of the Magnetic Field on the instability and observations?

We will begin with the standard assumptions commonly used in basic astrophysical systems. Once established, we will gradually lift these constraints and expand upon them.

To start, let's first take a brief detour into flows, approximations, fluid instabilities and finally Rayleigh-Taylor Instability (RTI).

1.1 Flows of Ideal Fluids

In this section, we will give an overview of several aspects of fluid flow, starting with ideal fluids. So, the simplest approximation is to ignore all the dissipative processes and take **entropy** of the system to be constant.

$$\frac{Ds}{Dt} = \frac{\partial s}{\partial t} + \vec{v} \cdot \nabla s = 0 => \boxed{s = s(\rho, p)} \tag{1.1}$$

Now, **Euler equation** can be written as:

$$\frac{\partial \vec{v}}{\partial t} + (\vec{v} \cdot \vec{\nabla})\vec{v} = -\frac{\vec{\nabla} P}{\rho} + \vec{g} \tag{1.2}$$

where $\vec{v}$ is the velocity field of the fluid, P is the pressure and ρ is the fluid density. By modifying this equation by defining **vorticity** ($\vec{\Omega} = \nabla \times \vec{v}$), we get the final equation as:

$$\boxed{\frac{\partial \Omega}{\partial t} = \nabla \times (\vec{v} \times \vec{\Omega}) + \frac{1}{\rho^2}(\nabla \rho \times \nabla p)} \tag{1.3}$$

In addition to the above equation, the most fundamental equation is the **Continuity Equation**:

$$\boxed{\frac{\partial \rho}{\partial t} + \nabla \cdot (\rho \vec{v}) = 0} \tag{1.4}$$

These equations (1.1, 1.3, 1.4) provides a set of 5 equations for 5 variables: $\rho, P, \vec{v}$. To solve them, we need further approximations.

1.2 Fluid Approximations[4]

1.2.1 Barotropic Fluids:

In this case, pressure can be written in terms of density alone. So, $\vec{\nabla} p$ will be parallel to $\vec{\nabla} \rho$ then equation of flow becomes:

$$\frac{\partial \Omega}{\partial t} = \vec{\nabla} \times (\vec{v} \times \vec{\Omega}) \tag{1.5}$$

We can define a quantity, called **Circulation**, defined as the surface integral of *vorticity*;

$$\Gamma \equiv \int \vec{\Omega} \cdot d\vec{s} = \int (\vec{\nabla} \times \vec{v}) \cdot d\vec{s} = \oint \vec{v}.d\vec{l}$$

which is conserved in the flow[1].

1.2.2 Steady flow:

We know that steady flow condition is given as:

$$\frac{\partial \Phi}{\partial t} = 0 \tag{1.6}$$

where, Φ is any variable corresponding to fluid property.
In such cases, we can introduce the concept of streamlines, determined as follows:

$$\frac{dx}{v_x} = \frac{dy}{v_y} = \frac{dz}{v_z} \tag{1.7}$$

[1]For some contour $\mathcal{C}$, Γ shows same value as the contour moves through the fluid.

In steady flow, the streamlines do not change with time, and the tangent at each point shows the direction of velocity of fluid element. Also, both $\frac{ds}{dt}$ and $\frac{\partial s}{\partial t}$ are zero in this case, implying that s remains constant along each streamline.
From thermodynamics, we know that the enthalpy is given as:

$$dw = d\epsilon + pdV + Vdp = Tds - pdV + pdV + Vdp \tag{1.8}$$

$$\boxed{dw = \frac{1}{\rho}dp} \tag{1.9}$$

- For perfect gas: $w = \frac{\gamma p}{\rho}\frac{1}{(\gamma-1)}$
- For incompressible liquid: $\gamma \to \infty \Rightarrow w = \frac{p}{\rho}$

Using steady flow conditions, the Euler equation is written as:

$$\frac{\partial \vec{v}}{\partial t} - (\vec{v} \times \vec{w}) = -\frac{1}{2}\vec{\nabla}v^2 - \frac{1}{\rho}\vec{\nabla}p - \vec{\nabla}\phi \tag{1.10}$$

Taking curl on both sides,

$$\frac{1}{2}\nabla v^2 - (\vec{v} \times \vec{\Omega}) = -\frac{1}{\rho}\nabla p - \nabla\phi \tag{1.11}$$

where ϕ is gravitational potential. With some calculation, we reach to the **Bernoulli's Equation**:

$$\boxed{d\left(\frac{1}{2}v^2 + w + \phi\right) = 0} \tag{1.12}$$

An example of steady flow is **Hydrostatic Equilibrium**, where there is no actual flow ($\vec{v} = 0$), and the fundamental governing equations are

$$\nabla p = -\rho\nabla\phi \tag{1.13}$$
$$\nabla^2\phi = 4\pi G\rho \tag{1.14}$$

which for a non-rotating body in thermal equilibrium and spherical symmetry combine to form

$$\boxed{\frac{1}{r^2}\frac{d}{dr}\left(\frac{r^2}{\rho}\frac{d\phi}{dr}\right) = -4\pi G\rho} \tag{1.15}$$

For astrophysical context, if the system is assumed to be a polytropic, we can use the polytropic equation of state,

$$P = K\rho^\gamma \tag{1.16}$$

where K is a constant and $\gamma = 1 + \frac{1}{n}$ is the polytropic index.

1.2.3 Irrotational, Isoentropic Flow of Ideal Fluids:

For irrotational fluid, $\vec{\nabla} \times \vec{v} = 0$. So, we can take $\vec{v} = \vec{\nabla}\psi$, where ψ is a potential for velocity field. Using this in eq-1.10,

$$\vec{\nabla}\left(\frac{\partial \psi}{\partial t}\right) + \frac{1}{2}v^2 = -\frac{\vec{\nabla}p}{\rho} - \vec{\nabla}\phi \tag{1.17}$$

$$\frac{\partial \psi}{\partial t} + \frac{1}{2}v^2 + \omega + \phi = f(t) \tag{1.18}$$

where $f(t)$ is an arbitrary function of time. We can take it to be zero without any loss of generality, as we can always add an arbitrary function to ψ without changing $\vec{v} = \vec{\nabla}\psi$.

So,

$$\boxed{\frac{\partial \psi}{\partial t} + \frac{1}{2}v^2 + \omega + \phi = 0} \tag{1.19}$$

becomes the generalized time-dependent Bernoulli's equation.

1.2.4 Incompressible, Irrotational flow of Ideal Fluids:

These are the most drastic events, in which we take ρ = constant (due to incompressibility). So, we can take the case of barotropic fluid flow. With $\vec{\nabla} \cdot \vec{v} = 0$, we get the equation of fluid flow as

$$\frac{\partial}{\partial t}(\vec{\nabla} \times \vec{v}) = \vec{\nabla} \times [\vec{v} \times (\vec{\nabla} \times \vec{v})] \tag{1.20}$$

This equation can entirely be expressed in terms of velocity alone. Further, for irrotational flow, $\vec{\Omega} = 0$, hence for this case, ψ will satisfy the Laplace's equation: $\nabla^2\psi = 0$.

1.2.5 Magnetic Field Approximation

When studying magnetized RTI, a uniform magnetic field is assumed initially to analyze its stabilizing effects.

1.2.6 Boundary and Numerical Approximations

The numerical simulations use a finite-volume method for solving hydrodynamic equations. The study is done with 2D simulations for computational efficiency.

1.3 Fluid Instability

Depending on the physical context of the system, fluid motion shows a rich variety of instabilities. They can be very complex in nature, but to understand in the first place, we will only talk about linear stability analysis.
Considering a system, which is in equilibrium, when perturbed slightly, all the relevant equations can be linearised in terms of perturbed quantities. For such a linear system, we can use a well known solution: $e^{\iota(\omega t + kx)}$.

1.3.1 Rayleigh-Taylor Instability (RTI)

Let's consider two fluids with density ρ and ρ' as shown in figure. Considering the fluids to be at rest initially, if the interface is slightly distorted, we want to find whether it will lead to an instability, mixing of fluids or an stable wave propagation. Let's, give

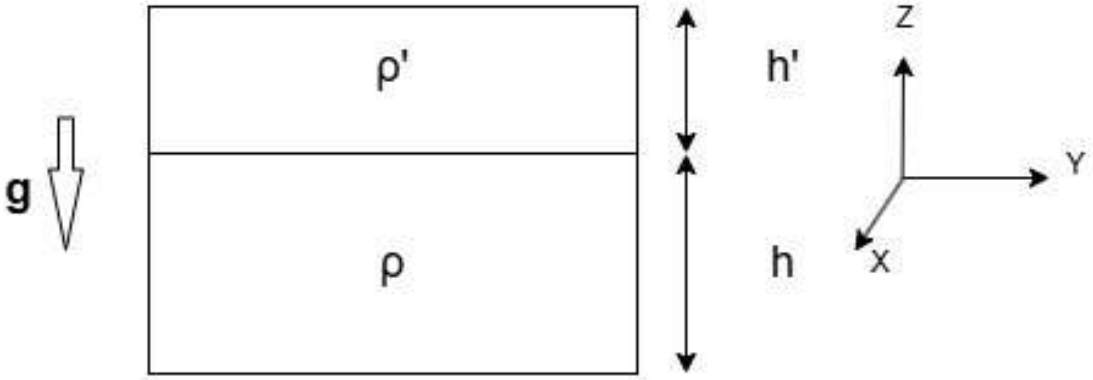

(a) Geometry of an instability.

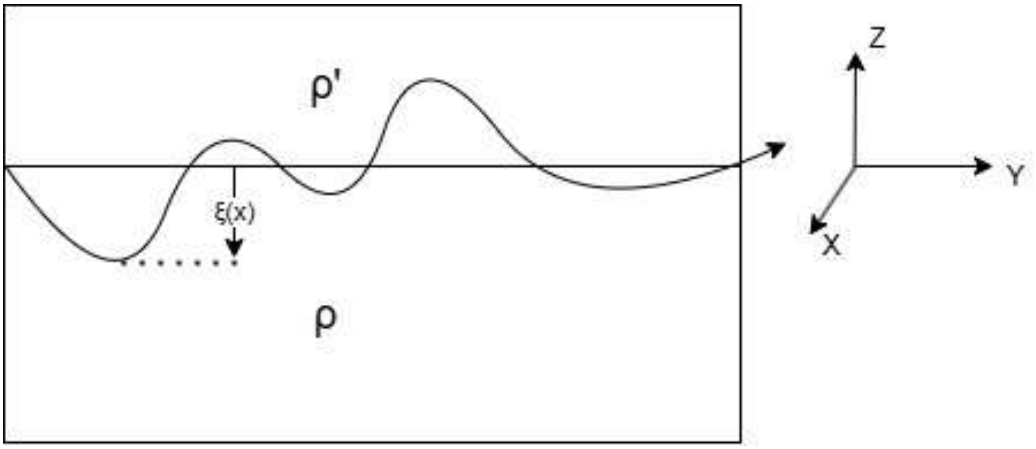

(b) Perturbation at the surface of discontinuity.

Figure 1.1

some disturbance to the system. As shown in figure-1.1b, let $\xi(x)$ be the displacement of surface in z-direction at coordinate x. As we are interested in only linear terms, the disturbances in velocity $\vec{v}$ will be $\vec{v} + \Delta\vec{v}$. So, we can ignore $(\vec{v} \cdot \vec{\nabla})\vec{v}$.

Considering an incompressible flow (i.e., $\omega = p/\rho$), from eq:1.18, we can write

$$\frac{\partial \psi}{\partial t} + \frac{p}{\rho} + gz = 0$$

$$\Rightarrow p = -\rho g z - \rho \frac{\partial \psi}{\partial t} \tag{1.21}$$

As, pressure should be continuous at the surface of separation $p(\xi(x)) = p'(\xi(x))$:

$$-\rho g \xi - \rho \frac{\partial \psi}{\partial t} = -\rho' g \xi - \rho' \frac{\partial \psi'}{\partial t}$$

$$(\rho' - \rho) g \xi = -\rho' \frac{\partial \psi'}{\partial t} + \rho \frac{\partial \psi}{\partial t}$$

$$\boxed{\xi(x) = \frac{1}{g(\rho - \rho')}\left[\rho' \frac{\partial \psi'}{\partial t} - \rho \frac{\partial \psi}{\partial t}\right]} \tag{1.22}$$

Another boundary matching condition is that the z-component of the velocity for each of the liquids should be same, i.e.; $\vec{v} = \vec{\nabla}\psi = \vec{\nabla}\psi' = \vec{v'}$:

$$\boxed{\frac{\partial \psi}{\partial z} = \frac{\partial \psi'}{\partial z}} \tag{1.23}$$

Finally, to the first order approximation, z-component of velocity can also be written as the time derivative of displacement $\xi(x)$. Using eq;1.22:

$$\boxed{\frac{\partial \xi(x)}{\partial t} = \frac{1}{g(\rho - \rho')}\left[\rho' \frac{\partial^2 \psi'}{\partial t^2} - \rho \frac{\partial^2 \psi}{\partial t^2}\right]} \tag{1.24}$$

For incompressible fluid, $\nabla^2 \psi = 0$. Substituting a solution $\psi = f(z)\cos(kx - \omega t)$:

$$\frac{\partial^2 \psi}{\partial x^2} + \frac{\partial^2 \psi}{\partial z^2} = 0$$

$$\implies -k^2 f(z)\cos(kx - \omega t) + \cos(kx - \omega t)\frac{d^2 f}{dz^2} = 0$$

$$\implies \frac{d^2 f}{dz^2} - k^2 f(z) = 0$$

This is a standard second order differential equation, with the general solution given by,

$$f(z) = Ae^{kz} + Be^{-kz}$$

where A and B are constants which are to be determined by boundary conditions. Then,

$$\psi = (Ae^{kz} + Be^{-kz})\cos(kx - \omega t) \tag{1.25}$$

[2] Further, the velocity field has to vanish at the top and the bottom surfaces, that is, at $z = h'$ and $z = -h$. These conditions lead to the equations:

$$Ae^{kh'} - Be^{-kh'} = 0 \implies A = Be^{-2kh'}$$

$$Ae^{-kh} - Be^{kh} = 0 \implies B = Ae^{2kh}$$

This leads to the solution,

$$\psi = A\cosh k(z + h)\cos(kx - \omega t) \tag{1.26}$$

$$\psi' = B\cosh k(z - h')\cos(kx - \omega t) \tag{1.27}$$

Substituting these into eq:1.24, at z = 0 we get,

$$g(\rho - \rho')Ak\sinh kh\cos(kx - \omega t) = -\rho'\omega^2 B\cosh kh'\cos(kx - \omega t) + \rho\omega^2 A\cosh kh\cos(kx - \omega t)$$

$$\implies g(\rho - \rho')Ak\sinh kh + \rho'\omega^2 B\cosh kh' = \rho\omega^2 A\cosh kh$$

[2] Here the ω is known as the Angular Growth Rate of the perturbation. The linear growth rate can be calculated by multiplying ω with $2\pi/\lambda$.

Dividing by A,

$$g(\rho - \rho')k\sinh(kh) + \frac{B}{A}\rho'\omega^2\cosh(kh') = \rho\omega^2\cosh(kh)$$

Also, from equation (1.23),

$$\frac{B}{A} = \frac{\sinh kh}{\sinh kh'}$$

After equating the ratio of B/A from these two equations, we get the dispersion relation,

$$\boxed{\omega^2 = \frac{kg(\rho - \rho')}{\rho\coth kh + \rho'\coth kh'}} \tag{1.28}$$

which determines the properties of the perturbation.
For the equilibrium to be stable we need, $\omega^2 > 0 \implies \rho > \rho'$. In this case, the dispersion relation describes gravity waves propagating at the interface between two liquids. The following limiting forms of this dispersion relation are of interest:

- First, if we take $\rho' = 0$, we get

$$\omega^2 = gk\tanh kh \tag{1.29}$$

  which is the dispersion relation for gravity waves propagating on the surface of a fluid of depth h

  - When the depth is very large ($kh \gg 1$), this reduces to

$$\omega^2 = gk\tanh kh \tag{1.30}$$

  - Whereas for $kh \ll 1$ we get,

$$\omega^2 = k^2gh \tag{1.31}$$

  These two limits are called deep-water waves and shallow-water waves. The shallow-water waves are non-dispersive ($\omega \propto k$), making the phase velocity $v_{ph} = \omega/k$ the same as the group velocity $v_g \equiv d\omega/dk$ whereas deep-water waves are dispersive.

- Second, when $\rho' \neq 0$, we still have three limiting cases.

  - For $kh \gg 1$ and $kh' \gg 1$ (with both liquids very deep),

$$\omega^2 = \frac{kg(\rho - \rho')}{\rho + \rho'} = -kgA \tag{1.32}$$

[3]

  - For $kh \ll 1$ and $kh' \ll 1$ (long waves)

$$\omega^2 = \frac{k^2g(\rho - \rho')hh'}{\rho h' + \rho' h} \tag{1.33}$$

[3] $A = \frac{\rho' - \rho}{\rho' + \rho}$ is known as the **Atwood's Number** and quantifies the change in density across the fluid interface. For physical systems, $0 \leq A < 1$. Higher A values leads to a more unstable interface and faster RTI growth.

– For $kh \gtrsim 1$ and $kh' \ll 1$

$$\omega^2 = \frac{k^2 g h'(\rho - \rho')}{\rho} \tag{1.34}$$

Our results show that the equilibrium is unstable if $\rho < \rho'$, that is, if the *heavier liquid is residing on top of the lighter liquid*. This is the **Rayleigh-Taylor instability**. In general, Rayleigh-Taylor instability occurs whenever $d\rho/dz$ is positive and the gravity is acting downwards. In such a configuration, the system can lower the potential energy by moving the heavier liquid downwards; this is the physical origin of this instability.

1.4 Origin of RTI in the context of Astrophysics

In stars, this instability occurs in several scenarios, including supernova explosions, stellar convection zones, and accretion processes.

1.4.1 Supernova Explosions

When a massive star reaches the end of its life, its iron core collapses under gravity, forming a neutron star or black hole. This collapse releases an enormous amount of energy in the form of a shock wave that propagates outward. The outer layers of the star, which are less dense, are accelerated by the shock wave. Behind the shock, the inner layers (which are denser) move outward and push against the lighter outer layers, creating a density inversion, which is the main condition for RTI. Small perturbations at the interface between the heavier and lighter layers grow exponentially, forming the characteristic mushroom-like plumes seen in RTI.

1.4.2 Stellar Convection Zones

In stars, convection zones are the regions where energy is transported by the bulk motion of plasma rather than by radiation. These regions often involve density inversions, where heavier fluid (denser plasma) overlies a lighter one due to variations in temperature, composition, or phase transitions.

1.4.3 Accretion Disks and Binary Stars

Accretion disks are rotating structures of gas, dust, and plasma that form around massive objects such as black holes, neutron stars, and protostars. RTI can develop in these disks due to unstable density gradients and external forces acting on the disk material.

Chapter 2

Methodology

In this study, we employ analytical linear stability analysis of the Rayleigh–Taylor instability under various magnetic field and density profiles. The procedure is as follows:

1. **Governing Equations**: Begin with the ideal magnetohydrodynamic (MHD) equations—continuity, momentum (including gravity and Lorentz force), induction, and incompressibility—perturbing around an equilibrium state $(\rho_0, p_0, \mathbf{B}_0)$.

2. **Linearization**: Decompose each field into equilibrium and small perturbation components, e.g.

$$\begin{aligned}\rho(\mathbf{x},t) &= \rho_0(z) + \rho_1(\mathbf{x},t),\\ \mathbf{v}(\mathbf{x},t) &= \mathbf{0} + \mathbf{v}_1(\mathbf{x},t),\\ \mathbf{B}(\mathbf{x},t) &= \mathbf{B}_0(z) + \mathbf{B}_1(\mathbf{x},t),\\ p(\mathbf{x},t) &= p_0(z) + p_1(\mathbf{x},t).\end{aligned}$$

3. **Normal Mode assumptions**: Assume perturbations vary as $\exp[i(kx - \omega t)]$, reducing the problem to ordinary differential equations in z for each case:

- Case I: $\rho_0(z) \propto z^3$, $\mathbf{B}_0(z) \propto e^z$.
- Case II: ρ_0 constant, $\mathbf{B}_0(z) \propto e^z$.
- Case III: both ρ_0 and $\mathbf{B}_0$ constant.

4. **Boundary Conditions**: Enforce decay or continuity of vertical velocity perturbations u_z as $z \to \pm\infty$ (or at finite interfaces) to determine allowable eigenfunctions.

5. **Dispersion Relations**: Solve the resulting Sturm–Liouville problem to obtain analytical dispersion relations $\omega^2(k)$ and growth rates $\gamma = \mathrm{Im}(\omega)$. Key results:

- For constant profiles: $\gamma^2 = A_t g k - v_A^2 k^2$ with threshold $\omega_{\mathrm{th}}^* = \sqrt{A_t}$.
- For exponential field/density: obtain generalized expressions for $\gamma(k)$ by evaluating matrix determinants.

6. **Dimensionless Parameters**: Introduce normalized quantities ($k^* = kL_D$, $\omega^* = \omega/\omega_{pe}$, A_t) to compare stability across cases.

7. **Visualization**: Plot γ^2 versus k (and k^2) for each case using Python/Matplotlib, annotating threshold and fastest-growing modes.

Chapter 3

Analysis

3.1 Stabilization of magneto-RTI with non-uniform density and magnetic field [2]

The fluid is subjected to a static external magnetic field. The analysis considers incompressible fluids within this magnetic environment, neglecting effects such as viscosity, surface tension, and heat transfer. These fluids are governed by the equations of ideal magneto-hydrodynamics (MHD).
The ideal MHD equations are written as follows:

$$\rho\frac{\partial \mathbf{v}}{\partial t} = -\nabla p + \rho\mathbf{g} + \frac{1}{\mu_0}(\nabla \times \mathbf{B}) \times \mathbf{B} \tag{3.1}$$

$$\nabla \cdot \mathbf{v} = 0 \tag{3.2}$$

$$\frac{\partial \mathbf{B}}{\partial t} = \nabla \times (\mathbf{v} \times \mathbf{B}) \tag{3.3}$$

$$\frac{\partial \rho}{\partial t} + (\mathbf{v} \cdot \nabla)\rho = 0 \tag{3.4}$$

The quantities v, p, B, and ρ show velocity vector, thermal pressure, magnetic field vector, and density, respectively.
Now we consider small perturbations around the equilibrium state as follow:

$$p = p_0 + p_1, \quad \rho = \rho_0 + \rho_1, \quad \mathbf{B} = \mathbf{B}_0 + \mathbf{B}_1, \quad v = v_0 + v_1.$$

Here, v_0, p_0, $\mathbf{B}_0$, and ρ_0 are the equilibrium states of velocity, pressure, magnetic field, and density, respectively. Moreover, $\mathbf{v}_1$, p_1, $\mathbf{B}_1$, and ρ_1 are the perturbed terms of velocity, pressure, magnetic field, and density, respectively. While $\mathbf{v}_1 = (v_{x1}, v_{y1}, v_{z1})$, $\mathbf{B}_1 = (B_{x1}, B_{y1}, B_{z1})$, $\mathbf{g} = (0, 0, -g)$, and the fluid is arranged in the horizontal direction, the density is only a function of the vertical coordinate $z(\rho_0 = \rho_0(z))$, and $\mathbf{B}_0 = B_{x0}(z)\mathbf{e}_x + B_{z0}(z)\mathbf{e}_z$.

After substituting these perturbed quantities into the MHD equations, we get the following equations (upto linear order):

$$\rho_0\frac{\partial \mathbf{v}_1}{\partial t} = -\nabla p_1 + \rho_1\mathbf{g} + \frac{1}{\mu_0}\left[(\nabla \times \mathbf{B}_0) \times \mathbf{B}_1 + (\nabla \times \mathbf{B}_1) \times \mathbf{B}_0\right] \tag{3.5}$$

$$\nabla \cdot \mathbf{v}_1 = 0 \tag{3.6}$$

$$\frac{\partial \mathbf{B}_1}{\partial t} = \nabla \times (\mathbf{v}_1 \times \mathbf{B}_0) \tag{3.7}$$

$$\frac{\partial \rho_1}{\partial t} + (\mathbf{v}_1 \cdot \nabla)\rho_0 = 0 \tag{3.8}$$

Now we assume that the perturbation for each physical quantity in the xy- plane is exponential as follows:

$$\psi = f(z)\, e^{i(kx-\omega t)} \tag{3.9}$$

In this relation, k is the wave-number. ω is the frequency of perturbations or the rate of system departure from the equilibrium state and it may be complex in the overall quantitative state,

$$\omega = \omega_r + i\gamma$$

Then,

$$\partial_t \to -i\omega, \quad \nabla \to ik + \hat{z}\frac{d}{dz}$$

We use normal mode analysis and this leads to a general differential equation in the z component of velocity (u_z),

$$\begin{aligned}\frac{B_{z0}^2(z)}{\mu_0}\frac{d^4u_{z1}}{dz^4} + \frac{1}{\mu_0}\left\{4B_{z0}(z)\left(\frac{dB_{z0}(z)}{dz}\right) + 2ik_xB_{x0}(z)B_{z0}(z)\right\}\frac{d^3u_{z1}}{dz^3} \\ + \left\{\rho_0\omega^2 + D\right\}\frac{d^2u_{z1}}{dz^2} + \left\{\omega^2\left(\frac{d\rho_0}{dz}\right) + E\right\}\frac{du_{z1}}{dz} \\ - k^2\left\{\rho_0\omega^2 - F + g\left(\frac{d\rho_0}{dz}\right)\right\}u_{z1} = 0\end{aligned} \tag{11}$$

where the coefficients are:

$$\begin{aligned}D = \frac{1}{\mu_0}\Bigg\{ - k_x^2B_{x0}^2(z) + 3B_{z0}(z)\frac{d^2B_{z0}(z)}{dz^2} + 2\left(\frac{dB_{z0}(z)}{dz}\right)^2 - k^2B_{z0}^2(z) \\ + 3ik_x\left[B_{x0}(z)\frac{dB_{z0}(z)}{dz} + B_{z0}(z)\frac{dB_{x0}(z)}{dz}\right]\Bigg\}\end{aligned} \tag{12}$$

$$\begin{aligned}E = \frac{1}{\mu_0}\Bigg\{ - 2k_x^2B_{x0}(z)\frac{dB_{x0}(z)}{dz} + B_{z0}(z)\frac{d^3B_{z0}(z)}{dz^3} + \frac{dB_{z0}(z)}{dz}\frac{d^2B_{z0}(z)}{dz^2} \\ - 2k^2B_{z0}(z)\frac{dB_{z0}(z)}{dz} + ik_x\Bigg[2B_{z0}(z)\frac{d^2B_{x0}(z)}{dz^2} - 2k^2B_{x0}(z)\frac{dB_{z0}(z)}{dz} \\ + 2\frac{dB_{x0}(z)}{dz}\frac{dB_{z0}(z)}{dz} + \frac{dB_{x0}(z)}{dz}\frac{d^2B_{z0}(z)}{dz^2}\Bigg]\Bigg\}\end{aligned} \tag{13}$$

$$\begin{aligned}F = \frac{1}{\mu_0}\Bigg\{k_x^2B_{x0}^2(z) + ik_x\left[\frac{1}{k^2}B_{z0}(z)\left(\frac{d^3B_{x0}(z)}{dz^3} + \frac{dB_{x0}(z)}{dz}\frac{d^2B_{x0}(z)}{dz^2}\right)\right. \\ \left. - B_{z0}(z)\frac{dB_{x0}(z)}{dz}\right]\Bigg\}\end{aligned} \tag{14}$$

A general solution of this equation is given by,

$$u_{z1} = \sin\left(\frac{n\pi}{h}z\right)\exp(\lambda z). \tag{3.10}$$

where λ is a constant.
Now we study three cases based on density and magnetic field profiles:

3.1.1 Variable density and variable magnetic field

We consider the initial density profile as a cubic function of z, and the static external magnetic field is taken to vary exponentially with height. These profiles are expressed as:

$$\rho_0(z) \propto z^3, \tag{20}$$

$$B_0(z) \propto e^z, \qquad 0 \le z \le h. \tag{21}$$

we are considering the horizontal and vertical components of Alfven velocity as,

$$v_{fx}^2 = \frac{B_{x0}^2}{\mu_0\rho_0}, v_{fz}^2 = \frac{B_{z0}^2}{\mu_0\rho_0} \tag{3.11}$$

Defining some dimensionless quantities:

$$\begin{aligned}
&\omega^{*2} = \frac{\omega^2}{\omega_{pe}^2}, \quad \omega_{fx}^{*2} = \frac{v_{fx}^2}{\omega_{pe}^2 L_D^2}, \quad \omega_{fz}^{*2} = \frac{v_{fz}^2}{\omega_{pe}^2 L_D^2}, \quad \lambda^{*2} = \lambda^2 L_D^2, \quad h^{*2} = \frac{h^2}{L_D^2}, \quad k^{*2} = k^2 L_D^2, \\
&g^* = \frac{g}{\omega_{pe}^2 L_D}, \quad \omega_{pe} = \sqrt{\frac{\rho_0 e^2}{m_e^2}}, \quad z^* = \frac{z}{L_D}.
\end{aligned} \tag{3.12}$$

Here, ω_{fx}^* and ω_{fy}^* are horizontal and vertical components of static external magnetic field. k^* is the normalized perturbation wave number relative to the spatial change rate (density gradient) and $\lambda^* = \lambda L_D$ is the normalized perturbation wavelength relative to the spatial change rate, where λ is a constant value ($\lambda = -(2L_D)^{-1}$). L_D is the density-scale length ($L_D = \rho/\nabla\rho$).

By taking into account $\omega = \omega_r + i\gamma$ and $\omega_r = 0$ (unstable oscillations), we obtain the square normalized growth rate:

$$\gamma^{*2} = \left\{ \begin{array}{l}
\left\{\lambda^{*4} + \left(\frac{n\pi}{h^*}\right)^4 - 6\lambda^{*2}\left(\frac{n\pi}{h^*}\right)^2 + 2\lambda^{*3} - 6\lambda^*\left(\frac{n\pi}{h^*}\right)^2 \right. \\
\quad \left. + \left(\frac{5}{4} - k^{*2}\right)\left(\lambda^{*2} - \left(\frac{n\pi}{h^*}\right)^2\right) + \lambda^*\left(\frac{1}{4} - k^{*2}\right)\right\}\omega_{fz}^{*2} \\
+ \left\{2\lambda^*\left(\lambda^{*2} - 3\left(\frac{n\pi}{h^*}\right)^2\right) + 3\left(\lambda^{*2} - \left(\frac{n\pi}{h^*}\right)^2\right)^2 \right. \\
\quad \left. + \lambda^*\left(\frac{5}{4} - 2k^{*2}\right)\left(\frac{1}{4} - k^{*2}\right)\right\} \\
\times \left(6\lambda^{*2} + 6\lambda^* - 2\left(\frac{n\pi}{h^*}\right)^2 + \left(\frac{5}{4} - 2k^{*2}\right)\right)^{-1} \\
\times \left[(2\lambda^* + 1)k_x^{*2}\omega_{fx}^{*2} - (2\lambda^* + 1)\left(2\lambda^{*2} + 2\lambda^* - 2\left(\frac{n\pi}{h^*}\right)^2 + \left(\frac{1}{4} - k^{*2}\right)\right)\omega_{fz}^{*2}\right. \\
\quad \left. - k_x^{*2}\omega_{fx}^{*2}\left(\lambda^{*2} - \left(\frac{n\pi}{h^*}\right)^2\right) - \lambda^* k_x^{*2}\omega_{fx}^{*2} + k^{*2}k_x^{*2}\omega_{fz}^{*2} - 3k^{*2}g^* z^{*2}\exp(-z^*)\right]
\end{array} \right\} \times \left[\begin{array}{l}
-\left\{2\lambda^*\left(\lambda^{*2} - 3\left(\frac{n\pi}{h^*}\right)^2\right) + 3\left(\lambda^{*2} - \left(\frac{n\pi}{h^*}\right)^2\right)\right. \\
\quad \left. + \lambda^*\left(\frac{5}{4} - 2k^{*2}\right) + \left(\frac{1}{4} - k^{*2}\right)\right\} \\
\times \left\{2\lambda^{*3}z^{*3}e^{-z^*} + 3z^{*2}e^{-z^*}\right\} \\
\times \left(6\lambda^{*2} + 6\lambda^* - 2\left(\frac{n\pi}{h^*}\right)^2 + \left(\frac{5}{4} - 2k^{*2}\right)\right)^{-1} \\
+ z^{*3}e^{-z^*}\left(\lambda^{*2} - \left(\frac{n\pi}{h^*}\right)^2\right) + 3\lambda^* z^{*2}e^{-z^*} - k^{*2}z^{*3}e^{-z^*}
\end{array} \right]^{-1} \tag{3.13}$$

3.1.2 Constant densities (ρ_1, ρ_2) and variable magnetic field

We consider densities to be constant but the magnetic field profile is exponential i.e $B_0(z) \propto e^z$.

The Alfvén speed is the characteristic speed at which transverse perturbations in a magnetized plasma propagate along the magnetic-field lines as defined in equation (3.11).

$$v_A \;=\; \frac{B}{\sqrt{\mu_0\,\rho}} \tag{3.14}$$

where

- B is the magnetic-field strength (in tesla),
- ρ is the mass density of the plasma (in kg/m^3),
- $\mu_0 \approx 4\pi \times 10^{-7}\,\mathrm{H/m}$ is the permeability of free space.

When two incompressible fluids of densities ρ_1 and ρ_2 are arranged one atop the other in a gravitational field g, the classical RTI growth rate for a perturbation of wavenumber k (in the absence of magnetic fields) is

$$\gamma^2 \;=\; A_t\,g\,k \quad \text{where} \quad A_t \equiv \frac{\rho_2 - \rho_1}{\rho_2 + \rho_1} \tag{3.15}$$

is the Atwood number.

A uniform horizontal magnetic field introduces a stabilizing Alfvén–wave tension term, so the dispersion relation becomes,

$$\gamma^2 \;=\; A_t\,g\,k \;-\; v_A^2\,k^2, \tag{3.16}$$

where v_A is the Alfvén speed (averaged across the interface).

The boundary between unstable ($\gamma^2 > 0$) and stable ($\gamma^2 < 0$) modes is the marginal point $\gamma = 0$. Setting $\gamma^2 = 0$ in (3.16) gives

$$0 = A_t\,g\,k - v_A^2\,k^2 \quad\Longrightarrow\quad v_A^2 = \frac{A_t\,g}{k}. \tag{3.17}$$

We introduce

$$\omega^* \;\equiv\; \frac{v_A\,k}{\sqrt{g\,k}} \;=\; \sqrt{\frac{v_A^2\,k}{g}}.$$

Substituting the marginal condition (3.17) yields

$$\omega^{*2} = \frac{v_A^2\,k}{g} = \frac{\left(A_t\,g/k\right)k}{g} = A_t \quad\Longrightarrow\quad \omega^*_{\mathrm{th}} = \sqrt{A_t}. \tag{3.18}$$

Hence the minimum (threshold) dimensionless magnetic–field frequency required to just suppress RTI is

$$\boxed{\omega^*_{\mathrm{th}} = \sqrt{\frac{\rho_2 - \rho_1}{\rho_2 + \rho_1}} = \sqrt{A_t}}.$$

Below this value the mode grows ($\gamma > 0$); above it the magnetic tension fully stabilizes that wavenumber.

3.1.3 Constant densities (ρ_1, ρ_2) and constant magnetic field

If we consider a simplified case when both the densities are constant and magnetic field is also constant then we get [5],

$$\gamma^2 = A_t g k - \frac{2(\mathbf{k} \cdot \mathbf{B_0})^2}{\mu_0(\rho_1 + \rho_2)} \tag{3.19}$$

For a perturbation with $\mathbf{k} \perp \mathbf{B}_0$, also known as an interchange mode, the growth rate is the same as the RTI without a magnetic field. However, for a perturbation with $\mathbf{k} \parallel \mathbf{B}_0$, known as an undular mode, the growth rate is

$$\boxed{\gamma^2 = A_t\, g k - \frac{2(k B_0)^2}{\mu_0(\rho_1 + \rho_2)}} \tag{3.20}$$

The undular mode has a critical wavelength

$$\lambda_c = \frac{4\pi B_0^2}{\mu_0 A_t(\rho_1 + \rho_2) g} \tag{3.21}$$

at which $\gamma = 0$. If $\lambda < \lambda_c$, $\gamma^2 < 0$, which implies that only perturbations with wavelength $\lambda > \lambda_c$ can grow. Equation (3.20) also shows that there is a fastest-growing wavelength, which is given by,

$$\lambda_m = \frac{8\pi B_0^2}{\mu_0 A_t(\rho_1 + \rho_2) g} = 2\lambda_c \tag{3.22}$$

and which corresponds to a maximum growth rate,

$$\gamma_m = \sqrt{\frac{g k(\rho_1 - \rho_2)}{2(\rho_1 + \rho_2)}}. \tag{3.23}$$

As evident from equation (3.20), the magnetic field enters the expression for the growth rate with a negative contribution. This implies that a stronger magnetic field tends to suppress the growth of Rayleigh-Taylor instability. Increasing B_0 increases the critical wavelength λ_c, thus reducing the range of unstable wavelengths. Therefore, magnetic fields play a stabilizing role in Rayleigh-Taylor instability and can be used as a mechanism to control or reduce the instability growth.

Chapter 4

Results

4.1 Region of Stability

Following contour plot shows the region of stability and instability as function of densities. The blue colour marked as neutral region is just added to separate out the colours of the contour map.

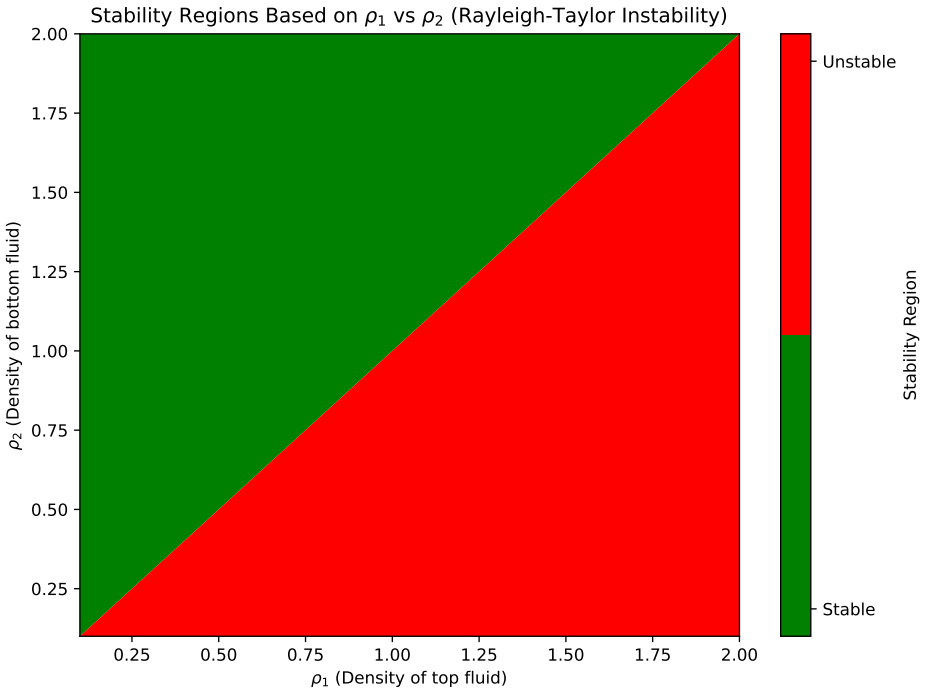

Figure 4.1: *Plot between ρ_1 vs ρ_2 showing stable and unstable region*

4.2 Effect of Magnetic field on instability/growth rate (γ^2)

4.2.1 Constant densities(ρ) and constant magnetic field (B_0)

Following graph demonstrates the trend of increasing magnetic field upon the growth rate γ^2. This shows that increasing magnetic field will increase the range of stable wavenumber (k) and decreases the range on stable wavelengths(λ). For $B = 0$ is forever unstable case. From the second figure we can see critical wavenumber (k_c) above which system will always remain stable. Also for k_{mid} which is equal to $\frac{k_c}{2}$ the growth rate becomes maximum.

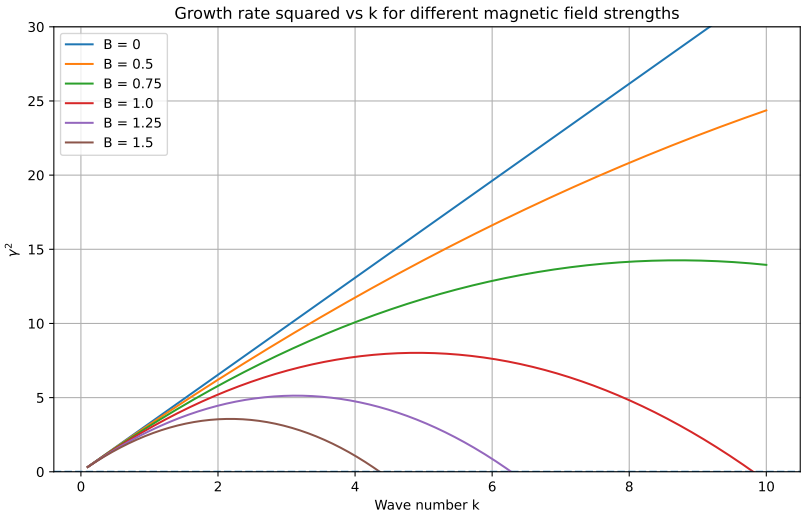

Figure 4.2: *Effect of increasing magnetic field B_0 on growth rate* (γ^2)

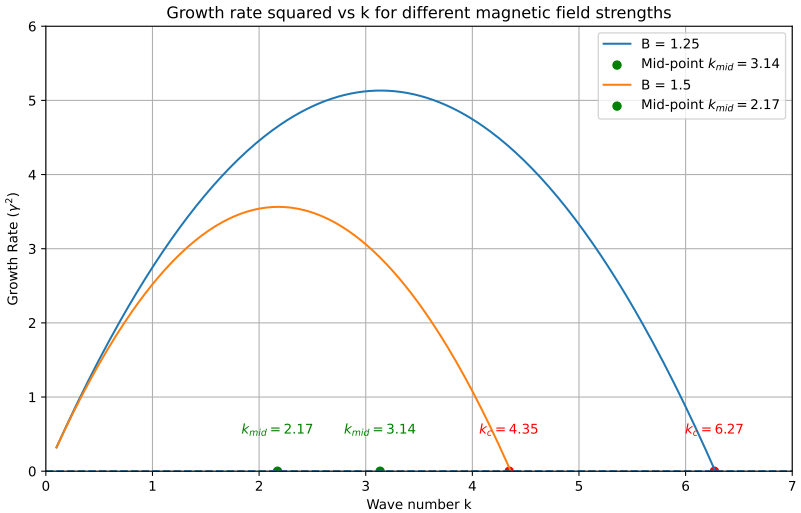

Figure 4.3: *Effect of increasing magnetic field B_0 on growth rate* (γ^2)

4.2.2 Constant densities (ρ) and exponential magnetic field ($B_0 e^z$)

Following graph demonstrates the trend of increasing magnetic field as result of increasing z, upon the growth rate γ^2. This shows that increasing magnetic field will increase the range of stable wavenumber (k) and decreases the range on stable wavelengths(λ) more faster than that of constant magnetic field as the field is exponential.

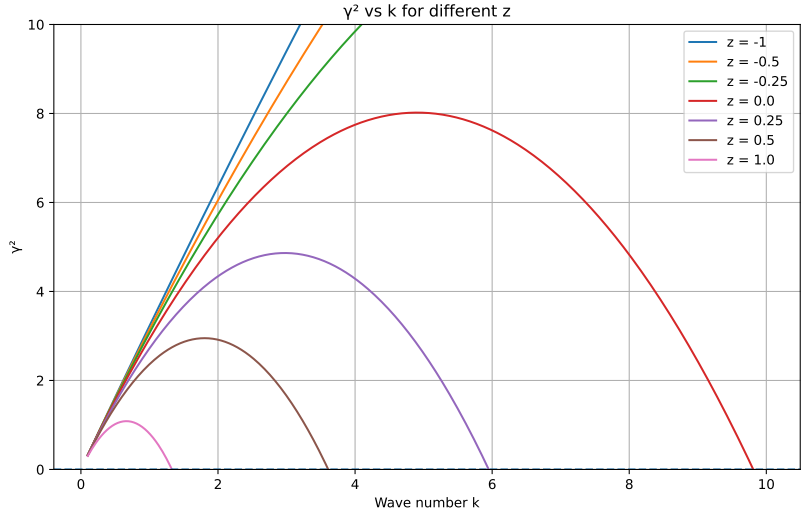

Figure 4.4: *Effect of increasing magnetic field B on growth rate* (γ^2)

4.2.3 Variable density ($\rho(z)$) and exponential magnetic field $B_0 e^z$

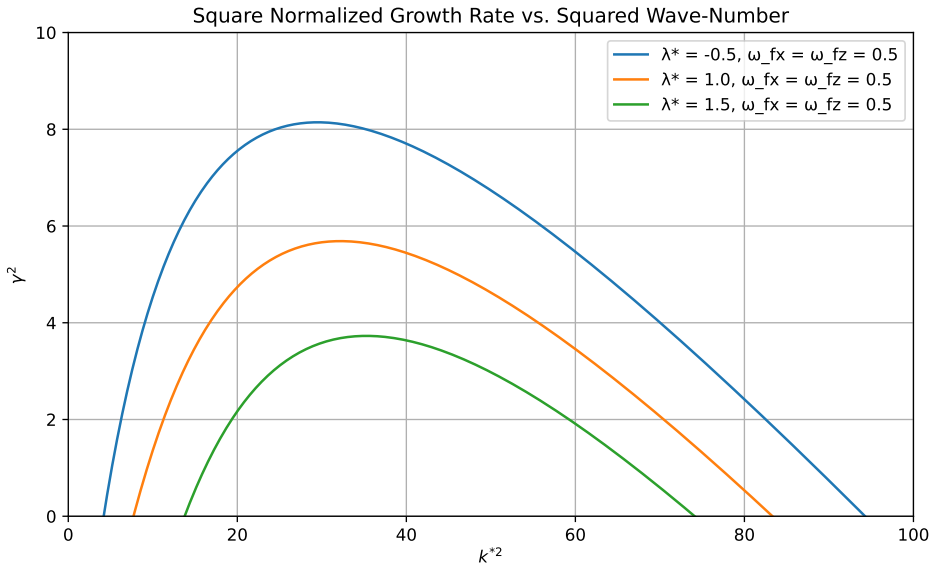

Figure 4.5: *Plot between* k^{*^2} *vs growth rate* (γ^2)

Chapter 5

Simulations

The simulation part will follow the FVM (Finite Volume Method). In this method the values at the centriod of the cell are calculated by using central difference (same as finite difference method), these values are then extrapolated to entire cells/'s faces using appropriate relations.

5.1 Finite Volume Method for the Compressible Euler Equations with Gravity

5.1.1 Principles of the Finite Volume Method

The finite volume method (FVM) is a discretisation technique for solving partial differential equations expressed in conservation form. Its key principles are:

- **Control Volumes**: The computational domain is partitioned into non-overlapping control volumes (cells). The solution is represented by average values over each control volume.
- **Conservation**: FVM enforces the integral form of conservation laws, ensuring that fluxes entering and leaving a control volume balance with sources and sinks within the cell.
- **Flux Evaluation**: Numerical fluxes are computed at cell interfaces using approximate or exact Riemann solvers, ensuring stability and accurately capturing discontinuities.
- **Reconstruction**: Higher-order accuracy is achieved by reconstructing variable profiles within each cell (e.g., linear or higher-degree polynomials) and applying slope limiters to avoid non-physical oscillations near discontinuities.
- **Source Terms**: When source terms (e.g., gravity) are present, operator splitting or well-balanced schemes are employed to maintain accuracy and preserve steady states.
- **Time Integration**: Explicit or implicit time-stepping schemes update the solution in time, adhering to stability constraints such as the Courant–Friedrichs–Lewy (CFL) condition.

5.1.2 Governing Equations

We solve the two-dimensional compressible Euler equations with a gravitational source term:

$$\frac{\partial \mathbf{U}}{\partial t} + \nabla \cdot \mathbf{F}(\mathbf{U}) = \mathbf{S}(\mathbf{U}, y), \tag{5.1}$$

where the conserved variables and fluxes are

$$\mathbf{U} = \begin{pmatrix} \rho \\ \rho v_x \\ \rho v_y \\ E \end{pmatrix}, \quad \mathbf{F}(\mathbf{U}) = \begin{pmatrix} \rho v_x & \rho v_y \\ \rho v_x^2 + p & \rho v_x v_y \\ \rho v_x v_y & \rho v_y^2 + p \\ (E+p)\, v_x & (E+p)\, v_y \end{pmatrix},$$

and the source term due to gravity g acting in the y-direction is

$$\mathbf{S}(\mathbf{U}, y) = \begin{pmatrix} 0 \\ 0 \\ \rho\, g \\ \rho\, v_y\, g \end{pmatrix}.$$

Here $p = (\gamma - 1)\big(E - \frac{1}{2}\rho(v_x^2 + v_y^2)\big)$, with γ the ratio of specific heats.

5.1.3 Finite Volume Discretization

Divide the domain into a uniform Cartesian mesh of cells of size $\Delta x = \Delta y$, with cell volumes $V = \Delta x^2$. Integrating over each cell and applying the divergence theorem gives the semi-discrete update:

$$\frac{d\mathbf{U}_{i,j}}{dt} = -\frac{1}{\Delta x}\Big(\mathbf{F}^x_{i+\frac{1}{2},j} - \mathbf{F}^x_{i-\frac{1}{2},j}\Big) - \frac{1}{\Delta y}\Big(\mathbf{F}^y_{i,j+\frac{1}{2}} - \mathbf{F}^y_{i,j-\frac{1}{2}}\Big) + \mathbf{S}_{i,j}\,. \tag{5.2}$$

5.2 Methodology [3]

The overall algorithm implemented in `finitevolume2.py` follows these steps:

1. **Grid Generation**: Construct a uniform $N \times 3N$ mesh and compute cell size Δx, cell volume V, and mesh coordinates (see `main()`).

2. **Initialization**: Assign initial primitive fields (ρ, v_x, v_y, p), including hydrostatic pressure and a sinusoidal velocity perturbation.

3. **State Conversion**: Use `getConserved` to form conserved variables $\mathbf{U}$; revert via `getPrimitive` after updates.

4. **Boundary Conditions**: Invoke `addGhostCells` and `setGhostCells` to enforce reflective and Dirichlet conditions at domain edges.

5. **Reconstruction**: Compute cell-centered gradients with `getGradient`, apply slope limiting via `slopeLimit`, and extrapolate to interfaces with `extrapolateInSpaceToFace`.

6. **Flux Computation**: Form numerical fluxes at each face using the Rusanov (local Lax–Friedrichs) solver in `getFlux`.

7. **Time Step Calculation**: Determine dt under the CFL constraint using local wave speeds (velocity + sound speed).

8. **Update**: Perform Strang splitting: half-step source update via `addSourceTerm`, full-step flux divergence update via `applyFluxes`, then final half-step source update.

9. **Iteration**: Repeat until t_{end} is reached; optional real-time plotting of the density field.

5.3 Implementation in `finitevolume2.py`

5.3.1 Mesh and Initialization

- **Grid:** `dx = boxsizeX/N`, `vol = dx**2`, and `X,Y = np.meshgrid(...)` set up a uniform $N \times 3N$ mesh in `main()`.
- **Initial Conditions:** A heavy fluid layer above a light one with a sinusoidal v_y perturbation; pressure is hydrostatic: `P = P0 + g*(Y-0.75)*rho`.

5.3.2 Conserved and Primitive Variables

- `getConserved` converts (ρ, v_x, v_y, p) to conservative $(M,\ Mv_x,\ Mv_y,\ E)$ via

$$M = \rho V, \quad E = \left(\tfrac{p}{\gamma-1} + \tfrac{1}{2}\rho(v_x^2 + v_y^2)\right)V$$

- `getPrimitive` inverts this: $\rho = M/V,\ v_x = M_x/(M),\ \ldots$ and recomputes p.

5.3.3 Boundary Conditions (Ghost Cells)

- `addGhostCells` pads the solution array in y by mirroring at top/bottom.
- `setGhostCells` enforces reflective v_y and constant ρ, v_x, p at those ghost rows.

5.3.4 Reconstruction and Slope Limiting

- `getGradient` computes centered differences via `np.roll` for each field gradient ∂_x, ∂_y.
- `slopeLimit` applies a minmod-type limiter to prevent new extrema.
- `extrapolateInSpaceToFace` reconstructs left/right states at each face:

$$f^L_{i+\frac{1}{2}} = f_i + \tfrac{1}{2}\Delta x\,(\partial_x f)_i, \quad f^R_{i+\frac{1}{2}} = f_{i+1} - \tfrac{1}{2}\Delta x\,(\partial_x f)_{i+1}$$

5.3.5 Numerical Flux: Local Lax–Friedrichs (Rusanov)

`getFlux` takes left/right states $\{\rho_{L,R}, v_{x,L,R}, v_{y,L,R}, p_{L,R}\}$ and computes

$$\mathbf{F}_{i+\frac{1}{2}} = \tfrac{1}{2}\big(\mathbf{F}(\mathbf{U}_L) + \mathbf{F}(\mathbf{U}_R)\big) - \tfrac{1}{2}\lambda_{\max}\,(\mathbf{U}_R - \mathbf{U}_L),$$

where $\lambda_{\max} = \max(|v_x| + c)$ is the largest local wave speed.

5.3.6 Time Integration and Source Splitting

- CFL-limited timestep: $dt = \text{CFL} \min_i \frac{\Delta x}{|v|+c}$
- Strang splitting for gravity via `addSourceTerm`:

$$E^* = E + \tfrac{1}{2}\, dt\, \rho v_y\, g, \quad (\rho v_y)^* = \rho v_y + \tfrac{1}{2}\, dt\, \rho\, g.$$

- Flux update via `applyFluxes`:

$$U_{i,j}^{n+1} = U_{i,j}^* - \frac{dt}{\Delta x}(F_{i+\frac{1}{2},j} - F_{i-\frac{1}{2},j}) - \frac{dt}{\Delta y}(G_{i,j+\frac{1}{2}} - G_{i,j-\frac{1}{2}}).$$

5.3.7 Main Time Loop

In `main()`, repeat the above until $t \geq t_{\text{end}}$, with optional density plotting via `matplotlib`.

This code is second-order in space (with slope limiting) and first-order in time (explicit Euler splitting).

References

[1] S. Chandrasekhar. "Hydrodynamic and Hydromagnetic Stability". In: *Hydrodynamic and Hydromagnetic Stability*. Chapter X: The Stability of Superposed Fluids – The Rayleigh-Taylor Instability. Oxford: Oxford University Press, 1961. Chap. 10, pp. 428–478.

[2] Mohammad-Ali Masoumparast Katek-Lahijani and Soheil Khoshbinfar. "Stabilization of magneto-Rayleigh-Taylor instability with non-uniform density and magnetic field profiles in Cartesian Geometry". In: *Chinese Journal of Physics* 91 (2024), pp. 479–493.

[3] Philip Mocz. *Create Your Own Finite Volume Fluid Simulation (With Python): Part 2 Boundary Conditions and Source Terms*. 2021. URL: https://github.com/pmocz/finitevolume2-python/tree/main.

[4] Thanu Padmanabhan. "Theoretical Astrophysics: Volume I – Astrophysical Processes". In: *Theoretical Astrophysics: Volume I – Astrophysical Processes*. Chapter 8: Fluid Instability. Cambridge: Cambridge University Press, 2000. Chap. 8, pp. 361–427.

[5] Yang Zhang, Pakorn Wongwaitayakornkul, and Paul M Bellan. "Magnetic Rayleigh–Taylor instability in an experiment simulating a solar loop". In: *The Astrophysical Journal Letters* 889.2 (2020), p. L32.